Special Issue

An Acute Injury Model for the Phenotypic Characteristics of Geographic Atrophy

Imran A. Bhutto,[1,2] Shuntaro Ogura,[1] Rajkumar Baldeosingh,[1] D. Scott McLeod,[1] Gerard A. Lutty,[1] and Malia M. Edwards[1]

[1]Department of Ophthalmology, Wilmer Eye Institute, Johns Hopkins Hospital, Baltimore, Maryland, United States
[2]Department of Ophthalmology, University of Pittsburgh, Pittsburgh, Pennsylvania, United States

Correspondence: Malia M. Edwards, Smith Building, Room M023, 400 North Broadway, Baltimore, MD 21231, USA; medwar28@jhmi.edu.

IAB and SO contributed equally to the work presented here and should therefore be regarded as equivalent authors.

Submitted: March 1, 2018
Accepted: August 7, 2018

Citation: Bhutto IA, Ogura S, Baldeosingh R, McLeod DS, Lutty GA, Edwards MM. An acute injury model for the phenotypic characteristics of geographic atrophy. *Invest Ophthalmol Vis Sci*. 2018;59:AMD143–AMD151. https://doi.org/10.1167/iovs.18-24245

Purpose. Geographic atrophy (GA) is the late stage of non-neovascular age-related macular degeneration. A lack of animal models for GA has hampered treatment efforts. Presented herein is a rat model for GA using subretinal injection of sodium iodate ($NaIO_3$).

Methods. Rats were given subretinal injections of $NaIO_3$ (5 μg/μL) using a pico-injector. Fundus photographs and spectral domain optical coherent tomography scans were collected at 1, 3, 7, 14, and 28 days after injection, at which time rats were euthanized and eyes were enucleated. Eyes were either cryopreserved or dissected into retinal and choroidal flatmounts. Fluorescence immunohistochemistry was performed for retinal glial fibrillary acidic protein (activated Müller cells and astrocytes) and vimentin (Müller cells), as well as peanut agglutin lectin (photoreceptors) labeling. RPE/choroids were labeled for RPE65 and CD34. Images were collected on Zeiss confocal microscopes.

Results. Fundus photos, spectral domain optical coherent tomography, and RPE65 staining revealed well-demarcated areas with focal loss of RPE and photoreceptors in $NaIO_3$-treated rats. At 1 day after injection, RPE cells appeared normal. By 3 days, there was patchy RPE and photoreceptor loss in the injected area. RPE and photoreceptors were completely degenerated in the injected area by 7 days. A large subretinal glial membrane occupied the degenerated area. Choriocapillaris was highly attenuated in the injected area at 14 and 28 days.

Conclusions. The rat model reported herein mimics the photoreceptor cell loss, RPE atrophy, glial membrane formation, and choriocapillaris degeneration seen in GA. This model will be valuable for developing and testing drugs and progenitor cell regenerative therapies for GA.

Keywords: age-related macular degeneration, geographic atrophy, choriocapillaris, retinal pigment epithelium, sodium iodate

Age-related macular degeneration (AMD) is one of the most common irreversible causes of severe central vision loss in the population older than 65 years.[1] AMD is a heterogenous disease, which first manifests in the macula with the appearance of pigmentary changes and subretinal deposits called drusen. In the dry, nonexudative form, AMD leads to geographic atrophy (GA) of the RPE and choriocapillaris (CC) along with photoreceptor degeneration. The etiology of GA remains poorly understood. Furthermore, there is a distinct lack of animal models to study GA disease pathogenesis and treatment efficacy.

Although dietary supplements reduce the disease progression to some extent, there is no proven drug treatment for GA. Regenerative cell therapy may provide some hope, but models for testing this are lacking. For this reason, a well-characterized, cost-effective, and rapid degeneration animal model of GA would be very useful. Sodium iodate ($NaIO_3$) injection has been extensively used as a preclinical model of RPE degeneration and GA.[2–5] Different delivery routes and various doses of $NaIO_3$ have been reported to induce RPE changes in a variety of mammalian species.[2–7] $NaIO_3$ is thought to directly affect the RPE cells with secondary effects on photoreceptors and the CC. It has been shown to induce the production of reactive oxygen species contributing to damage similar to human GA.[8–11] The current models using systemic delivery of $NaIO_3$, however, result in widespread degeneration. The degeneration is not succinct and is not surrounded by healthy retina and choroid, as seen in human GA.

This study aimed to improve on the current $NaIO_3$ model by creating a rat model with a well-circumscribed area of RPE atrophy, CC attenuation, and photoreceptor degeneration bordered by healthy full-thickness retina and choroid adjacent to the subretinal site of $NaIO_3$ injection.

Materials and Methods

Animals

Adult male Brown Norway (Charles River Labs) pigmented rats (6 to 8 weeks old) were used. Rats were housed in a 12-hour light and 12-hour dark cycle and fed water and dried ration ad libitum. Rats were divided into two groups: one group received subretinal injections of $NaIO_3$ and the other group of animals (sham group) received PBS injections. Experimental procedures were approved by the Animal Care and Use Committee of the Johns Hopkins University (Baltimore, MD, USA). Rats were cared for and used in compliance with the statement for the

Use of Animals in Ophthalmic and Vision Research by the Association for Research in Vision and Ophthalmology.

$NaIO_3$ Preparation and Subretinal Injection

$NaIO_3$ (S-4007; Sigma-Aldrich, St. Louis, MO, USA) was dissolved in PBS to a concentration of 5 mg/mL. Rats received a single subretinal injection of sterile $NaIO_3$ (1 μL) or PBS in each eye. Subretinal injections were performed using sterilized glass micro needles back-filled with injection solution and connected to a controlled pressure delivery device (PLI-100 Pico-Injector; Harvard Apparatus, Holliston, MA, USA) as previously described.[12] Eyes showing massive subretinal or vitreous hemorrhage were excluded from analysis.

Fundus Photography, Fluorescein Angiography, and Optical Coherence Tomography

Fundus images were obtained at 1, 3, 7, 14, and 28 days using a Micron III retinal-imaging microscope for rodents (Phoenix Research Labs, Pleasanton, CA, USA) equipped with a CCD camera. For fluorescein angiography (FAG), 50 μL 10% fluorescein sodium (100 mg/mL) was injected intravenously, and images were captured on the Micron III. Optical coherence tomography (OCT) was performed on anesthetized rats using a spectral domain OCT system (Leica Microsystems, Buffalo Grove, IL, USA) adapted for small animals. Pupils were dilated with 1% tropicamide and 2.5% phenylephrine eye. Each image was obtained with a scanning mode of 2.6 × 2.6 × 1.4 mm, 1000 A-scans × 100 B-scans, and averaged to remove random noise from the final images. Scans were taken in the same rats at 1, 3, 7, 14, and 28 days after subretinal injection of $NaIO_3$ ($n = 4$). Additional rats were also analyzed at each time point until their endpoint (total animals at each time point: day 1, 13; days 3, 7, 11; day 14, 7; day 28, 4). PBS-injected controls were also imaged ($n = 6$). Retinal thickness was compared with controls at each time point using Student *t*-tests.

Immunohistochemistry on Retinal and RPE/Choroidal Flatmounts

Rats were euthanized at 1, 3, 7, 14, and 28 days after injection. Eyes were enucleated and processed for either flatmount immunohistochemistry or cryopreserved ($n = 3$ at each age cryopreservation and flatmount). For flatmount histology, the retinas separated from the RPE/choroid complex. Tissues were fixed in 2% paraformaldehyde (PFA) in Tris-buffered saline (TBS) at 4°C overnight. The flatmount retinas were blocked in 5% goat serum (prepared in TBS with 0.1% Triton X-100 + 1% BSA) for 5 hours before incubation in primary antibodies overnight at 4°C. Retinas were incubated in chicken anti–glial fibrillary acidic protein (GFAP; activated Müller cells and astrocytes; 1:500; Millipore, Burlington, MA, USA) and rabbit anti-vimentin (Müller cells; 1:200, ab45939; Abcam, Inc., Cambridge, MA, USA), whereas RPE/choroid eyecups were stained with mouse anti-RPE65 (1:200; NB100-355, Novus Biologics, Littleton, CO, USA) and rabbit anti-CD34 (1:200; ab81289; Abcam, Inc.). After washes, tissues were incubated in secondary antibodies (goat anti-rabbit Alexa Fluor 647 [A21244; Invitrogen, Waltham, MA, USA], goat anti-chicken cyanine 3 [105-165-155; Jackson Immunoresearch, West Grove, PA, USA], and goat anti-mouse cyanine3 [115-165-003; Jackson Immunoresearch]) overnight. FITC-conjugated peanut agglutin lectin (PNA; 1:500; Sigma) was added to the secondary antibody cocktail for retinas. Flatmounts were imaged using Zeiss 510 or 710 Meta confocal microscopes equipped with Zen software (Carl Zeiss, Thornwood, NY, USA).

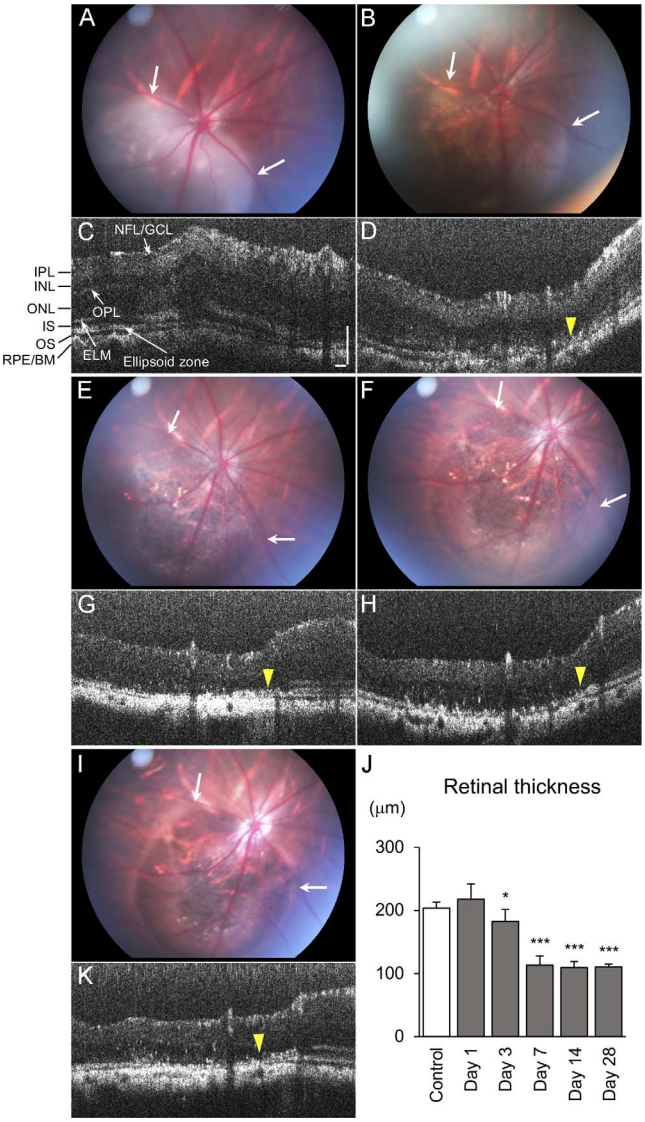

Figure 1. Sequential monitoring of the same eye with fundus photograph and spectral domain OCT scans at 1 (**A**, **C**), 3 (**B**, **D**), 7 (**E**, **G**), 14 (**F**, **H**), and 28 (**I**, **K**) days after $NaIO_3$ injection. Note the area of retinal atrophy was observed at 1 day and did not expand with time (*arrows*). A distinct transition zone is observed between nonaffected retina and damaged retina after day 3, where the RPE/Bruch's membrane complex is irregular and discontinuous, and retinal thinning is observed (*yellow arrowhead*). (**J**) The graph shows retinal thickness after injection, indicating thinning was observed at day 3, and the atrophy was completed by day 7. *Error bars* denote SD (control, $n = 6$; day 1, $n = 13$; days 3, 7, $n = 11$; day 14, $n = 4$; day 28, $n = 4$; $^{*}P < 0.05$, $^{***}P < 0.001$; two-tailed Student's *t*-test). *Scale bars* indicate 100 μm (NFL, nerve fiber layer; GCL, ganglion cell layer; IPL, inner plexiform layer; INL, inner nuclear layer; OPL, outer plexiform layer; ONL, outer nuclear layer; IS, inner segment; ELM, external limiting membrane; OS, outer segment; BM, Bruch's membrane).

Histologic Assessment

Cryoblocks were cut into 8-μm sections, and sections were stained with hematoxylin and eosin (H&E).

Results

$NaIO_3$ concentrations ranging from 2 mg to 40 mg/mL were injected into the subretinal space to determine the optimal

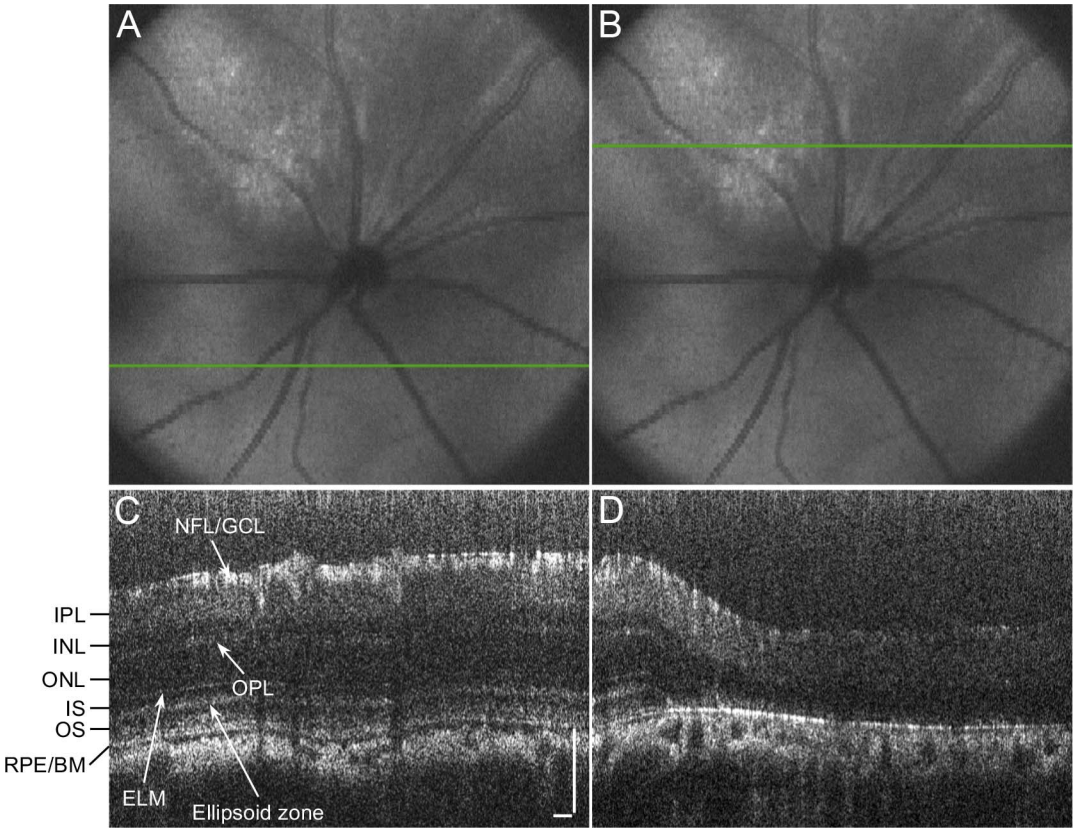

Figure 2. Spectral domain OCT scans at 14 days after subretinal injection of $NaIO_3$. (**A**, **C**) The retina outside the affected area appeared preserved having all retinal layers. (**B**, **D**) The retinal thinning is apparent in the scan within the injured area, with deterioration of the ellipsoid zone and the RPE/Bruch's membrane complex. *Scale bars* indicate 100 μm.

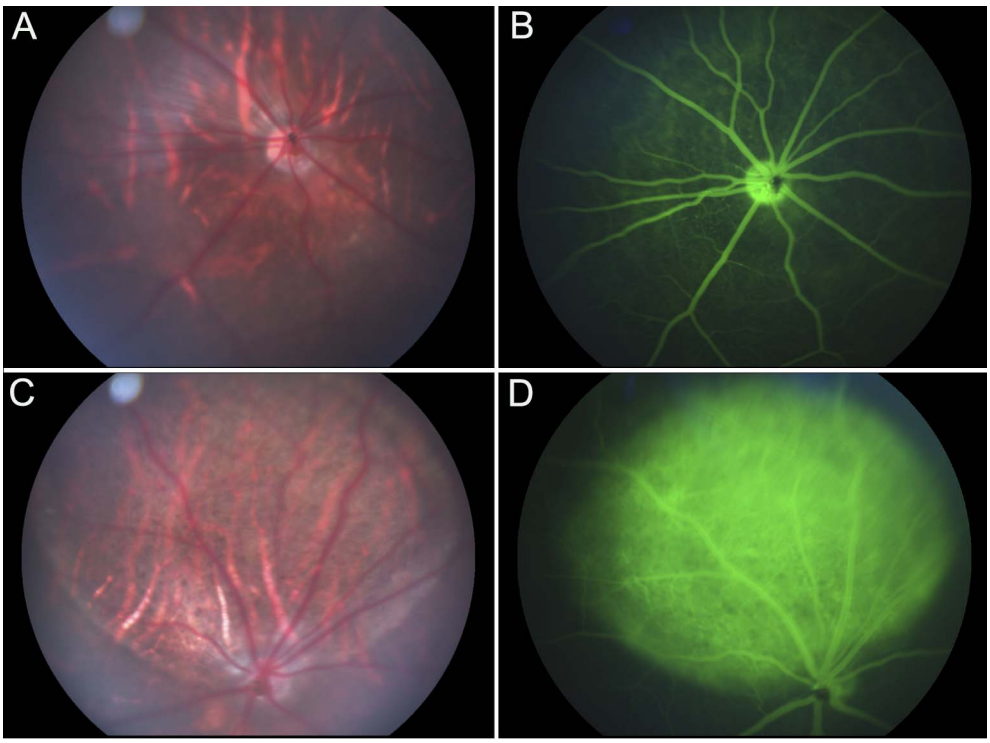

Figure 3. Fundus photograph and FAG of eyes receiving PBS (**A**, **B**) or (**C**, **D**) $NaIO_3$ injections. (**A**, **B**) Eyes receiving PBS injections remained normal even at day 28. (**C**, **D**) At 7 days after injection, aberrant FAG staining of the CC is apparent in the injected area of $NaIO_3$-treated eyes.

Investigative Ophthalmology & Visual Science

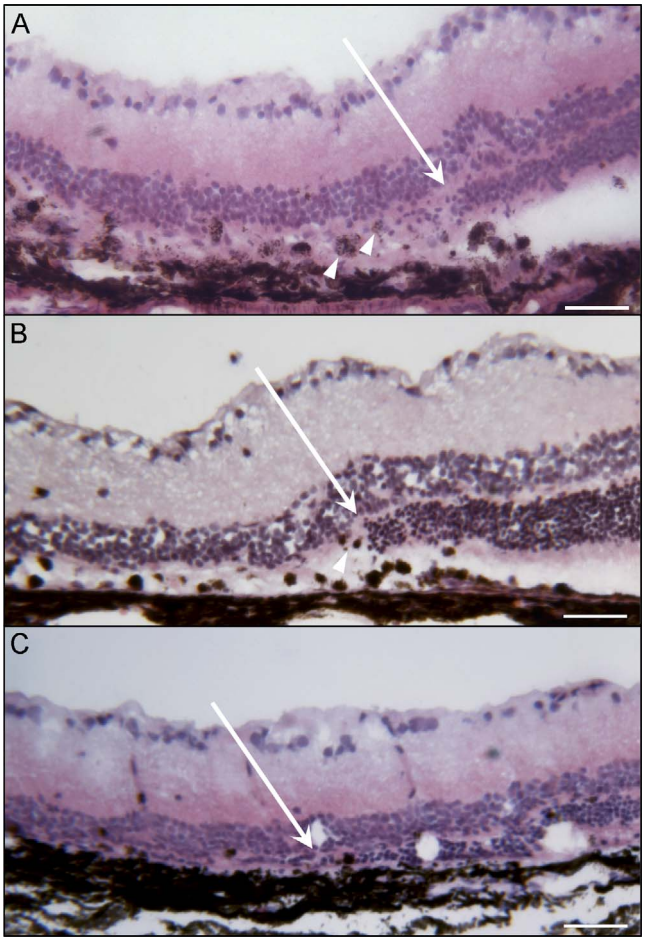

Figure 4. H&E staining of cryosections at (**A**) 3, (**B**) 7, and (**C**) 28 days after $NaIO_3$ injection. A transition from preserved retina (*right*) to the damaged retina with the ONL disappearing (*arrow*) is clearly observed after subretinal $NaIO_3$ at all time points. At the transition zone, hypertrophic, spherical RPE cells are evident at days 3 and 7 (*arrowheads*). Selective damage of outer retinal layers within the induced lesion is quite visible histologically. At 28 days, the retina in the bleb area has collapsed into the subretinal space. *Scale bars* indicate 50 μm.

dose for producing a well-defined area of RPE atrophy. The 2 mg/mL dose induced a partial but slow progressive RPE degeneration within the bleb area and no CC changes at 28 days (data not shown). Doses greater than 20 mg/mL produced severe and rapid RPE and CC loss (data not shown). The 5 mg/mL dose was chosen for this study because it produced well-circumscribed and demarcated atrophic area with RPE and photoreceptor loss followed by CC loss at later time points.

Eyes were clinically assessed by fundus and OCT examination at 1, 3, 7, 14, and 28 days after injection. PBS-injected eyes had a normal appearing fundus at all ages. OCT imaging of these eyes revealed a small elevation of the retina at 1 day after injection, which returned to normal at 3 days. This area remained normal through 28 days (Supplementary Fig. S1). To best monitor the progression of RPE atrophy resulting from subretinal $NaIO_3$, rats were imaged at all time points until their endpoint. At 1 day after injection, eyes receiving $NaIO_3$ had some retinal edema (Fig. 1A). This edema resulted in a slight increase in retinal thickness, measured by OCT, compared with controls at day 1 (Figs. 1C, 1J). By 3 days, the edema was resolved, and the area receiving $NaIO_3$ had some patchy RPE loss (Fig. 1B). OCT imaging demonstrated the retinal thickness was significantly lower than controls at 3 days (Figs. 1D, 1J). Fundus examination at 7 days revealed a clearly defined area with RPE loss (Fig. 1E). Outside the area where $NaIO_3$ was injected, the eyes remained normal (Fig. 1E). OCT examination also demonstrated thinning of the outer retinal layers in the injected area (Figs. 1G, 1J). The transition zone between nonaffected and affected areas was clearly defined. The fundus and OCT images were similar to 7 days at both 14 and 28 days (Figs. 1F, 1H–1K). Although evident in fundus photographs, the preservation of the retinal layers outside the injected area was confirmed by OCT scans (Fig. 2). The retinal thickness dropped significantly between 3 and 7 days but did not change between 7 and 28 days (Fig. 1J), indicating retinal atrophy was completed by day 7. All animals receiving good subretinal injections developed well-demarcated atrophic areas.

FAG revealed a normal retinal vascular pattern with no loss in inner or outer retinal barrier function in eyes injected with PBS (Figs. 3A, 3B). Eyes receiving $NaIO_3$ injection showed a window defect due to loss in the outer barrier at 7 days (Figs. 3C, 3D). This persisted at 14 and 28 days (data not shown).

Eyecups were sectioned and examined histologically at 3, 7, and 28 days (Fig. 4). At 3 days after injection, a clear area of RPE disruption and atrophy was apparent in cross section. This area was well demarcated with clear borders on both sides and a progressive loss of photoreceptors. Within this area, many RPE cells were absent, whereas others had migrated into the subretinal space and retina. Photoreceptor degeneration was also evident by loss of outer segments and thinning of the outer nuclear layer (ONL). In areas where RPE had migrated anteriorly, they often were multilayered and associated with displaced ONL (Fig. 4A). At 7 days after injection, the atrophic area remained well demarcated with a clear border. Within the injected area at this time point, RPE cells were almost completely missing from Bruch's membrane and photoreceptors were absent (Fig. 4B). At the border of atrophy, the RPE was hypertrophic and multilayered. The transition zone from atrophy to normal appearing retina was around 100 μm (Fig. 4). At 28 days after injection, the RPE layer, ONL, and external limiting membrane (ELM) were missing only in the injected area. There was still a clearly defined border between atrophic and normal retina (Fig. 4C). The inner nuclear layer was immediately adjacent to Bruch's membrane in the degenerated area.

Retinal flatmounts were viewed with the ELM en face. In PBS-injected controls, vimentin staining created a honeycomb-like ELM that covered the entire retina (data not shown). At 1 day after injection, the injected area was not evident in retinal flatmounts (data not shown). By 3 days, sporadic photoreceptor loss was observed, but vimentin and GFAP staining were unremarkable (data not shown). At days 7 through 28, the area receiving $NaIO_3$ was void of PNA-positive segments. GFAP and vimentin double-positive processes overlapped one another to create a membrane-like structure in the subretinal space where photoreceptors were lost (Fig. 5). As demonstrated in eye cups, this area had distinct borders between atrophy and normal area (Fig. 5A–5C). These membranes were the densest in the center (Fig. 5D–5F). This sharp border was even more prominent at higher magnification (Fig. 5G–5I).

RPE65 staining revealed a complete cobblestone monolayer pattern in control eyes. A similar pattern was observed in eyes from rats euthanized 1 day after $NaIO_3$-induced injury (Fig. 6A). At 3 days after injection, RPE65 staining of the RPE monolayer demonstrated patchy RPE cell loss, cellular ghosts, and a mottled appearance (Fig. 6B). At 7 days, there was a complete loss of RPE cells in the injected area, leaving only cell fragments and debris with RPE65 (Fig. 6C). This loss persisted at 14 and 28 days (Fig. 6D).

Investigative Ophthalmology & Visual Science

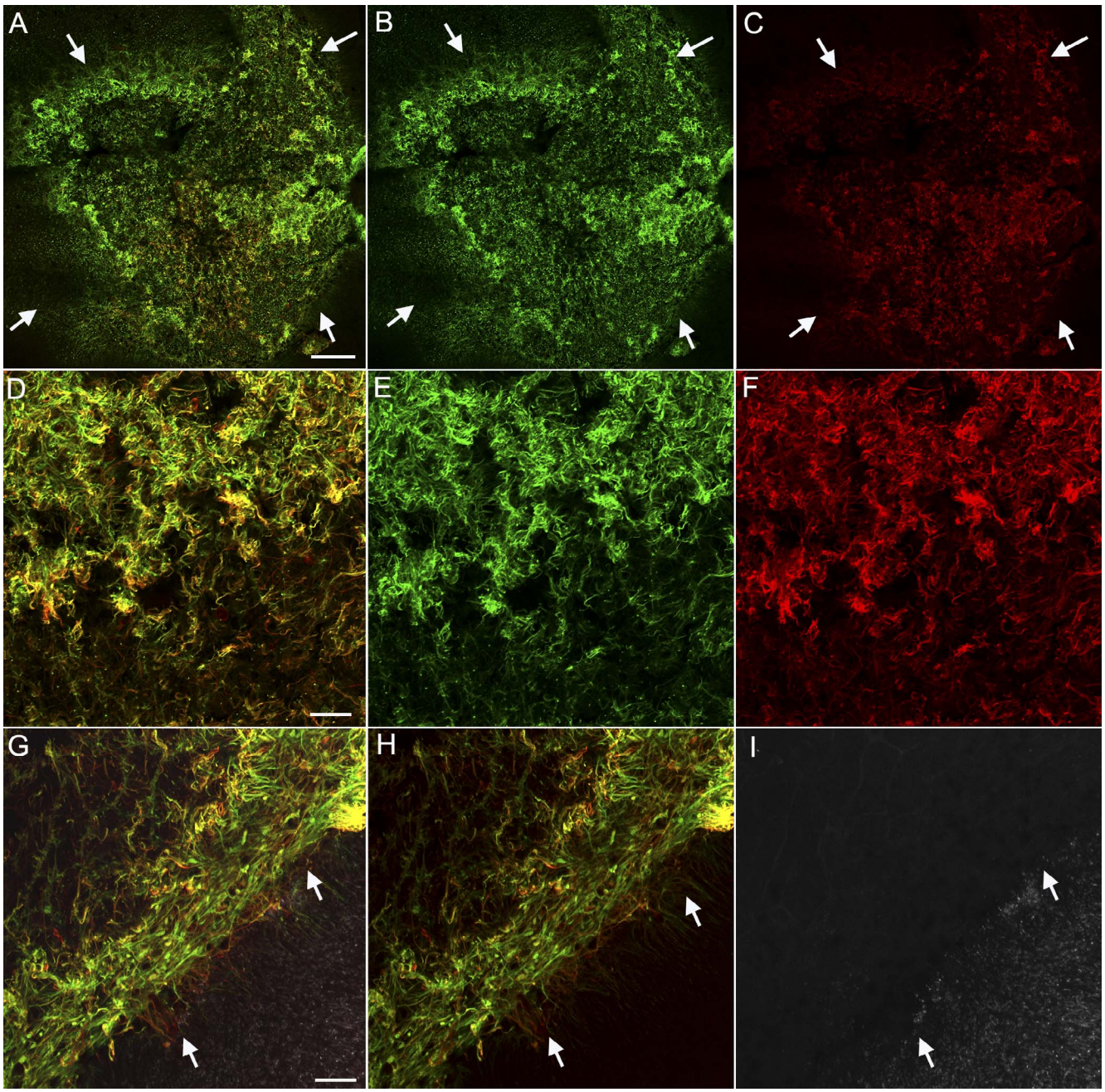

Figure 5. Flatmount retinas from rats 14 days after $NaIO_3$ subretinal injections were stained with GFAP (*red*), vimentin (*green*), and PNA (*white* in **G–I** only) and then imaged with the ELM en face. (**A–C**) Images of retinas at low magnification show GFAP and vimentin-positive cells extending through the ELM in the atrophic area (*arrows*). This area very closely matches that of RPE loss. A clear border is evident. (**D–F**) The center of this glial membrane shows processes positive for GFAP and vimentin, as well as single-positive cells and processes. (**G–I**) A clear border (*arrow*) is observed separating the area with a glial membrane but no PNA-positive segments from the remainder of the retina with intact photoreceptor segments (*white*, PNA). *Scale bars* indicate (**A–C**) 200 and (**D–I**) 50 μm.

The CC, stained with CD34, had a uniform, dense interconnecting pattern at day 1 after injection (Fig. 7A). At 3 and 7 days, the CC had a similar appearance with no apparent reduced density (Fig. 7B). The CC was severely attenuated at 14 days (Fig. 7C). Staining of the RPE/choroid with RPE65 and CD34 revealed the clear border where RPE atrophy was associated with CC attenuation (Fig. 7E). Further CC attenuation was noted at 28 days (Fig. 7D). The area of capillary attenuation perfectly matched that of RPE atrophy and the subretinal glial membrane (Fig. 8).

Discussion

Subretinally injected $NaIO_3$ created a reproducible rat model that mimics many aspects of GA. As in GA, the RPE atrophy preceded photoreceptor and CC loss, as well as glial membrane formation.[13–15] This model also develops a glial membrane which mimics that seen in eyes with GA.[16] The significance of this glial membrane is that it may prevent integration of photoreceptor progenitors in future regenerative medicine efforts. The rat model reported herein provides a

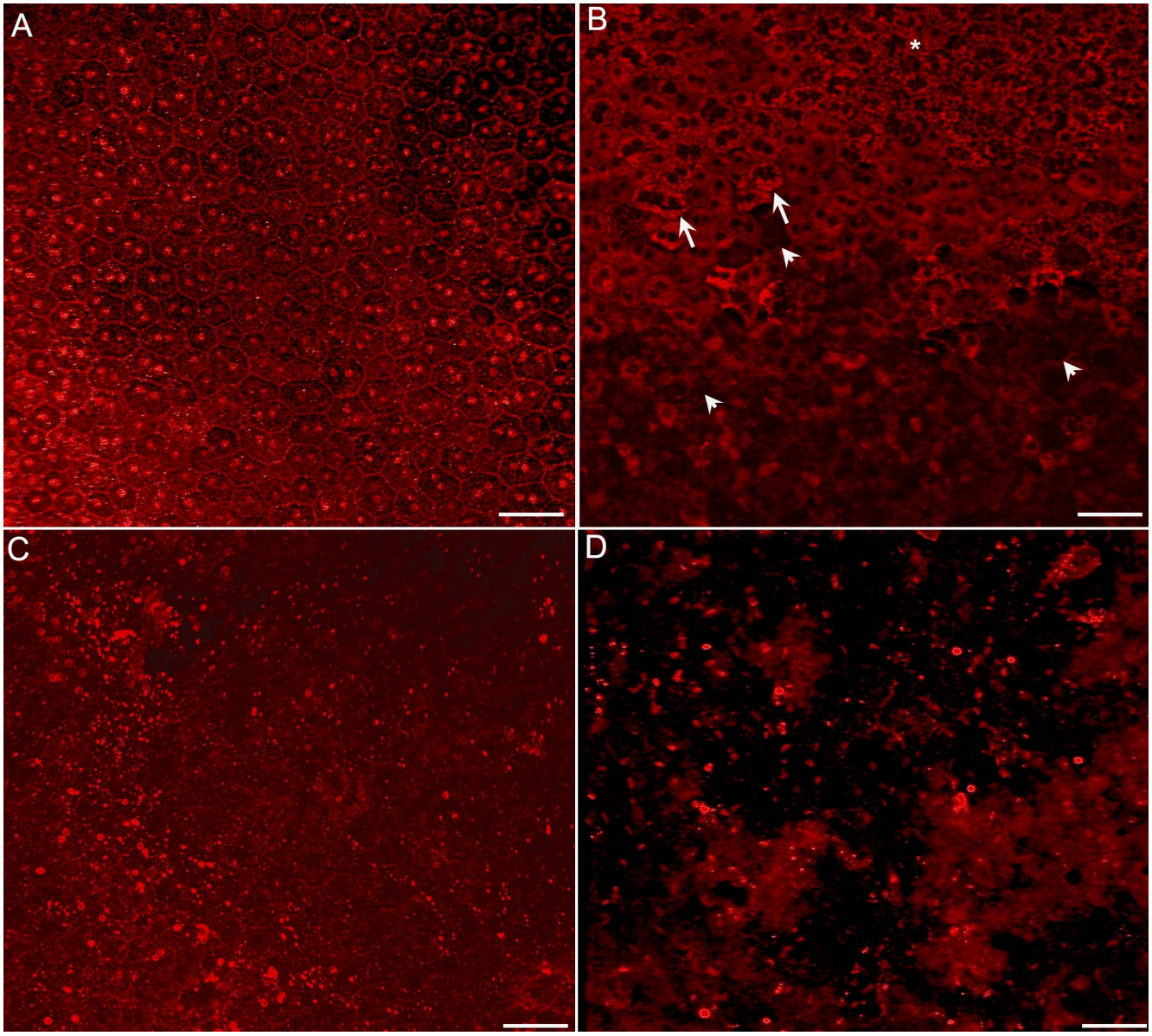

Figure 6. Flatmounts of RPE stained with RPE65. (**A**) At 1 day after injection, RPE65 staining clearly outlines the cell membranes, showing the hexagonal shape of the RPE cells. Cells are intact and healthy. (**B**) At 3 days after injection, some atrophic and hypertrophic (*arrows*) and mottled (*asterisk*) RPE cells are observed as are RPE ghosts (*arrowheads*). (**C**) At 7 days after injection, the RPE cells are completely lost with only fragments of cells remaining in the injected area. (**D**) At 28 days, only RPE fragments remain in the injected area. *Scale bars* indicate 50 μm.

rapid, novel avenue for testing drug therapy options for GA. This model may also be useful for evaluating human progenitor cells as regenerative medicine because the same pathology is observed when $NaIO_3$ is injected subretinally into athymic nude rats (Bhutoo IA, et al., *IOVS* 2017;58:ARVO E-Abstract 2289), which are partially immune suppressed.

The intravenous injection of $NaIO_3$ creates widespread RPE, photoreceptor, and CC atrophy.[2–5,17,18] This is in sharp contrast to the focal, succinct atrophic areas surrounded by intact, healthy RPE and CC seen in GA. The border region between atrophic and normal tissue is most interesting for studying disease progression of GA, as this is where degeneration is actively occurring. This region is not present with systemic injection of $NaIO_3$.

The rat model presented herein provides a succinct area of RPE/photoreceptor loss surrounded by healthy retinal tissue. The disease progression mimics that of GA with RPE cells lost first, followed by photoreceptors, and eventually, CC dropout. At 3 days after injection, before the complete loss of RPE cells, RPE cells were observed migrating anteriorly into the retina. Interestingly, anterior migrating RPE have recently been observed in eyes with AMD, and anterior migration is believed to contribute significantly to RPE loss in GA.[19–21] Similar anterior migration is also observed with retinal detachment. The descent of the ELM observed at the atrophic border in rats 7 days after injection is also reminiscent of that seen in humans with GA.[21] A subretinal glial membrane, similar to that recently reported in eyes with GA, was also observed in these rats.[16] Similar observations have been made when $NaIO_3$ was injected subretinally into rabbits and pigs.[6,7] In the rabbit model, however, a large volume (50 μL) was injected that created a significant bleb, and even the PBS-injected control eyes showed retinal and RPE changes.[6] Moreover, the rabbit retina is merangiotic (only partially vascularized), making it difficult

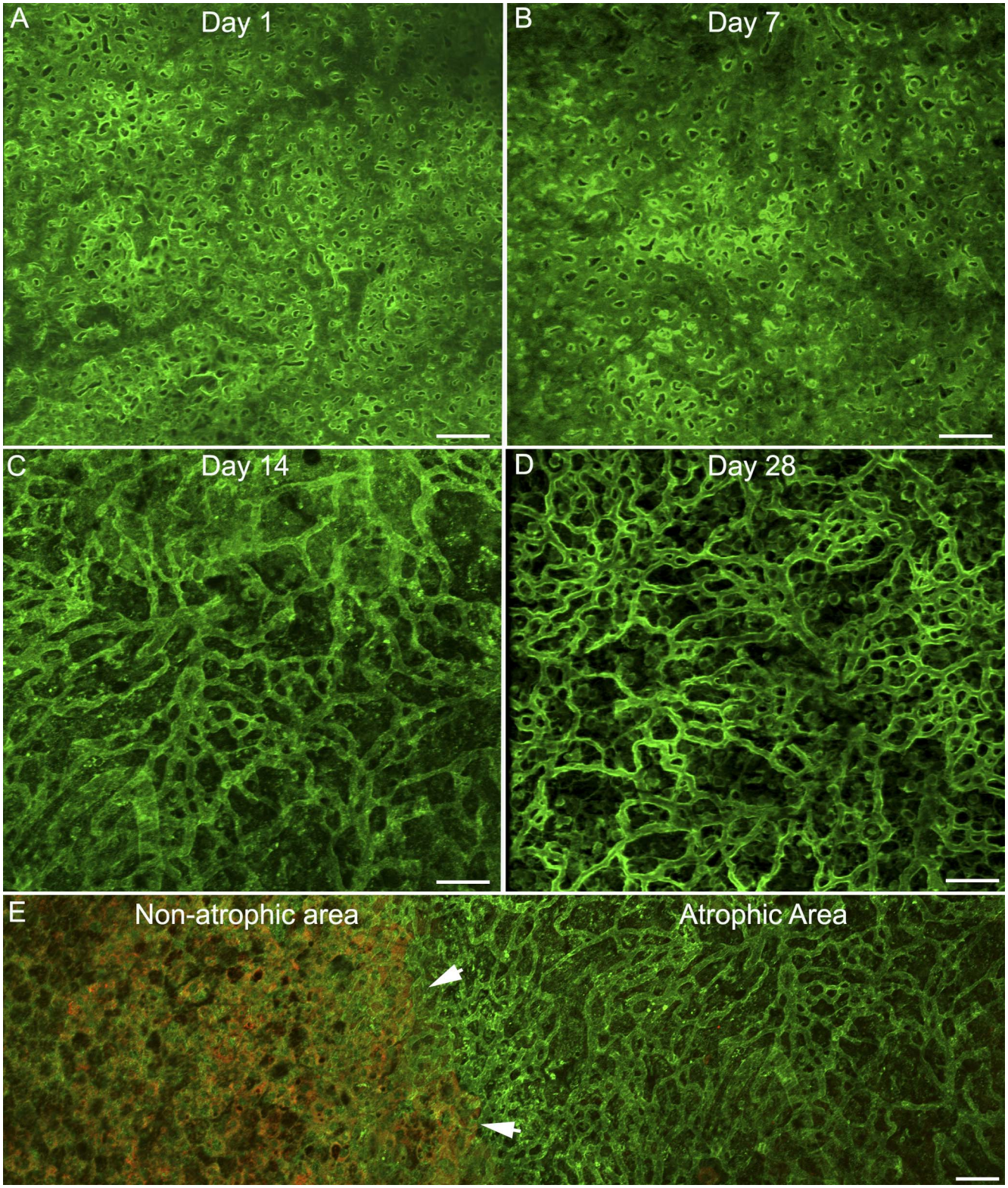

Figure 7. CD34 staining of CC demonstrates an intact network at days 1 (**A**) and 7 (**B**) after injection. (**C**) At 14 days after injection, CC attenuation was noted. (**D**) At 28 days, severe CC degeneration is apparent in the injected area. (**E**) RPE65 (*red*) and CD34 (*green*) costaining at 14 days shows the clear border (*arrowheads*) between atrophic and nonatrophic areas. *Scale bars* indicate 50 μm.

to translate results to a human disease, particularly one involving vascular changes. In the swine model, a much smaller dose (0.01 mg/mL) was sufficient to cause ONL and RPE cell loss while preserving the inner retina.[7] The lower dose required in swine compared with rats may be due to species differences. Although choroidal swelling was observed in the rabbit model, choroidal changes were not assessed in the other subretinal models. The attenuation of CC in rat but not in

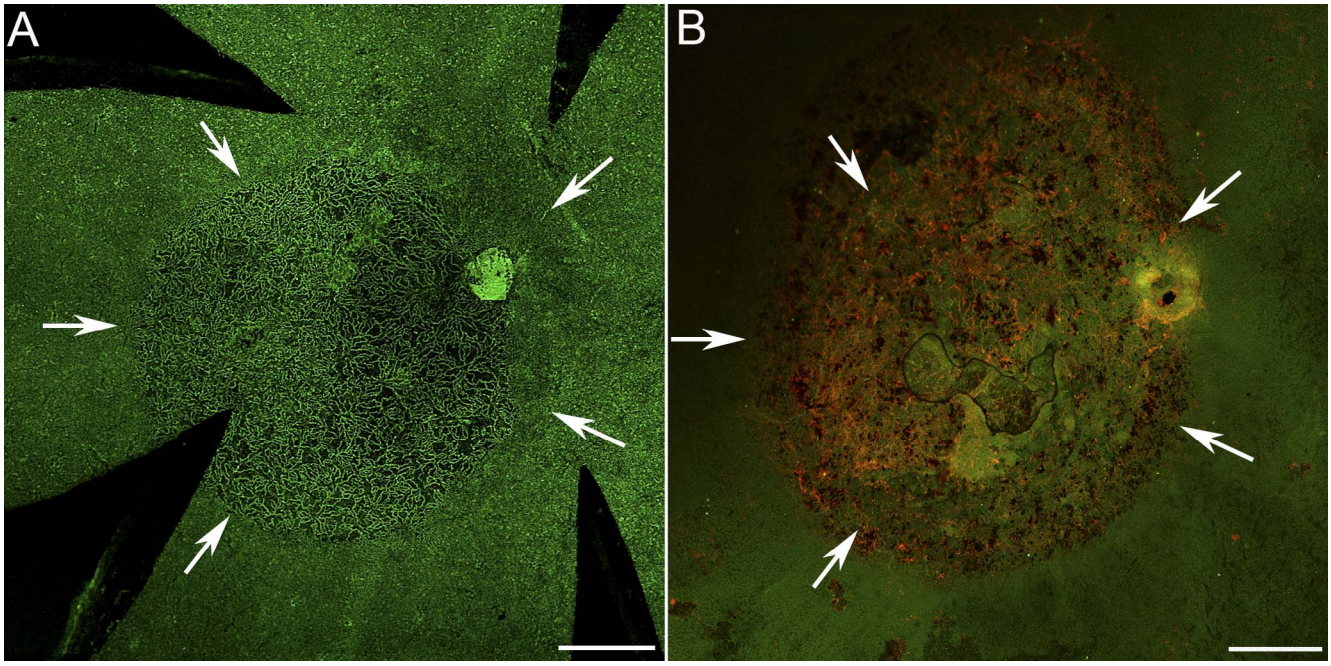

Figure 8. Low-magnification images of choroidal (**A**) and retinal flatmounts (**B**) at 28 days after injection show that the glial membrane closely mirrors the area of CC loss. *Arrows* indicate the atrophic area. *Scale bars* indicate 500 μm.

rabbit may be due to the incredible regenerative properties of rabbit CC.[22]

The CC loss in the model reported herein occurs after RPE and photoreceptor degeneration. This progression of atrophy mimics that seen in GA, with RPE loss preceding choroidal changes.[13,15] Some researchers have observed reduced blood flow in CC prior to RPE loss using angio-OCT.[23–25] Cross-sectional histologic analysis suggested that CC loss preceded RPE loss.[26] However, our flatmount histopathology, which provides a comprehensive analysis of the entire choroid, demonstrated that CC loss in eyes with GA only occurs in areas with no RPE cells.[13,15] Furthermore, viable capillaries in a fairly normal pattern were observed in areas lacking RPE.[13] One exception would be under drusen, where Mullins et al. observed loss of CC while RPE remained anterior to drusen.[24] The time between RPE loss and CC dropout provides a window of opportunity to treat RPE loss and possibly prevent CC loss. There is a need for therapeutic intervention for choroid because 50% of the CC is atrophic in the atrophic area in GA.[13–15]

One drawback of the rat model presented herein is that it is an acute injury model, and the mode of cell death is not the same as in GA. The $NaIO_3$-induced RPE loss may occur via oxidative stress, which is one factor believed to contribute to AMD pathology.[27] $NaIO_3$ is known to trigger oxidative stress, which is toxic to RPE cells.[8–11] Interestingly, both subretinal and systemic administration of $NaIO_3$ cause retinal edema at 1 day after injection. In both the model presented herein and previously reported systemic models, this edema is reduced by 3 and 7 days, respectively.[3] This suggests that the edema may result from $NaIO_3$-induced breakdown of the inner and outer retinal barriers.[28,29] In vitro experiments have shown that $NaIO_3$ decreased RPE migration and ZO1 expression.[30] Reduced barrier functions could also contribute to retinal thinning. The anterior migration of RPE observed herein and in human GA also contributes to outer barrier loss.

In conclusion, the subretinal injection of $NaIO_3$ in rats creates a reproducible and cost-efficient model for studying GA. Low dose injections produce succinct areas of photoreceptor and RPE loss, which leads to CC loss after 14 and 28 days. This model will be useful for developing and testing drug treatments and therapeutic interventions such as autologous iPSC or stem cell–derived tissue regenerative medicine for GA.

Acknowledgments

Supported by National Institutes of Health Grants EY016151 (GAL) and EY01765 (Wilmer Eye Institute), the Choroideremia Foundation, the Arnold and Mabel Beckman Foundation, the Altsheler-Durell Foundation, BrightFocus Foundation (MME), Foundation Fighting Blindness, and a Research to Prevent Blindness Unrestricted Grant (Wilmer Eye Institute).

Disclosure: **I.A. Bhutto**, None; **S. Ogura**, None; **R. Baldeosingh**, None; **D.S. McLeod**, None; **G.A. Lutty**, None; **M.M. Edwards**, None

References

1. Klein R, Klein BE. The prevalence of age-related eye diseases and visual impairment in aging: current estimates. *Invest Ophthalmol Vis Sci*. 2013;54:ORSF5–ORSF13.
2. Jian Q, Tao Z, Li Y, Yin ZQ. Acute retinal injury and the relationship between nerve growth factor, Notch1 transcription and short-lived dedifferentiation transient changes of mammalian Muller cells. *Vision Res*. 2015;110:107–117.
3. Chowers G, Cohen M, Marks-Ohana D, et al. Course of sodium iodate-induced retinal degeneration in albino and pigmented mice. *Invest Ophthalmol Vis Sci*. 2017;58:2239–2249.
4. Machalinska A, Kawa MP, Pius-Sadowska E, et al. Endogenous regeneration of damaged retinal pigment epithelium following low dose sodium iodate administration: an insight into the role of glial cells in retinal repair. *Exp Eye Res*. 2013;112:68–78.
5. Machalinska A, Lubinski W, Klos P, et al. Sodium iodate selectively injuries the posterior pole of the retina in a dose-dependent manner: morphological and electrophysiological study. *Neurochemical Res*. 2010;35:1819–1827.

6. Petrus-Reurer S, Bartuma H, Aronsson M, et al. Integration of subretinal suspension transplants of human embryonic stem cell-derived retinal pigment epithelial cells in a large-eyed model of geographic atrophy. *Invest Ophthalmol Vis Sci*. 2017;58:1314–1322.
7. Mones J, Leiva M, Pena T, et al. A swine model of selective geographic atrophy of outer retinal layers mimicking atrophic AMD: a phase I escalating dose of subretinal sodium iodate. *Invest Ophthalmol Vis Sci*. 2016;57:3974–3983.
8. Berkowitz BA, Bredell BX, Davis C, Samardzija M, Grimm C, Roberts R. Measuring in vivo free radical production by the outer retina. *Invest Ophthalmol Vis Sci*. 2015;56:7931–7938.
9. Wang J, Iacovelli J, Spencer C, Saint-Geniez M. Direct effect of sodium iodate on neurosensory retina. *Invest Ophthalmol Vis Sci*. 2014;55:1941–1953.
10. Xiao J, Yao J, Jia L, Lin C, Zacks DN. Protective effect of Met12, a small peptide inhibitor of Fas, on the retinal pigment epithelium and photoreceptor after sodium iodate injury. *Invest Ophthalmol Vis Sci*. 2017;58:1801–1810.
11. Yang Y, Qin YJ, Yip YW, et al. Green tea catechins are potent anti-oxidants that ameliorate sodium iodate-induced retinal degeneration in rats. *Sci Rep*. 2016;6:29546.
12. Baba T, Bhutto IA, Merges C, et al. A rat model for choroidal neovascularization using subretinal lipid hydroperoxide injection. *Am J Pathol*. 2010;176:3085–3097.
13. McLeod DS, Grebe R, Bhutto I, Merges C, Baba T, Lutty GA. Relationship between RPE and choriocapillaris in age-related macular degeneration. *Invest Ophthalmol Vis Sci*. 2009;50:4982–4991.
14. McLeod DS, Taomoto M, Otsuji T, Green WR, Sunness JS, Lutty GA. Quantifying changes in RPE and choroidal vasculature in eyes with age-related macular degeneration. *Invest Ophthalmol Vis Sci*. 2002;43:1986–1993.
15. Seddon JM, McLeod DS, Bhutto IA, et al. Histopathological insights into choroidal vascular loss in clinically documented cases of age-related macular degeneration. *JAMA Ophthalmol*. 2016;134:1272–1280.
16. Edwards MM, McLeod DS, Bhutto IA, Grebe R, Duffy M, Lutty GA. Subretinal glial membranes in eyes with geographic atrophy. *Invest Ophthalmol Vis Sci*. 2017;58:1352–1367.
17. Korte GE, Gerszberg T, Pua F, Henkind P. Choriocapillaris atrophy after experimental destruction of the retinal pigment epithelium in the rat. A study in thin sections and vascular casts. *Acta Anatomica*. 1986;127:171–175.
18. Yang Y, Ng TK, Ye C, et al. Assessing sodium iodate-induced outer retinal changes in rats using confocal scanning laser ophthalmoscopy and optical coherence tomography. *Invest Ophthalmol Vis Sci*. 2014;55:1696–1705.
19. Curcio CA, Zanzottera EC, Ach T, Balaratnasingam C, Freund KB. Activated retinal pigment epithelium, an optical coherence tomography biomarker for progression in age-related macular degeneration. *Invest Ophthalmol Vis Sci*. 2017;58:BIO211–BIO226.
20. Dolz-Marco R, Litts KM, Tan ACS, Freund KB, Curcio CA. The evolution of outer retinal tubulation, a neurodegeneration and gliosis prominent in macular diseases. *Ophthalmology*. 2017;124:1353–1367.
21. Zanzottera EC, Ach T, Huisingh C, Messinger JD, Freund KB, Curcio CA. Visualizing retinal pigment epithelium phenotypes in the transition to atrophy in neovascular age-related macular degeneration. *Retina*. 2016;36(Suppl 1):S26–S39.
22. Hayashi A, Majji AB, Fujioka S, Kim HC, Fukushima I, de Juan E Jr. Surgically induced degeneration and regeneration of the choriocapillaris in rabbit. *Graefes Arch Clin Exp Ophthalmol*. 1999;237:668–677.
23. Moreira-Neto CA, Moult EM, Fujimoto JG, Waheed NK, Ferrara D. Choriocapillaris loss in advanced age-related macular degeneration. *J Ophthalmol*. 2018;2018:8125267.
24. Mullins RF, Johnson MN, Faidley EA, Skeie JM, Huang J. Choriocapillaris vascular dropout related to density of drusen in human eyes with early age-related macular degeneration. *Invest Ophthalmol Vis Sci*. 2011;52:1606–1612.
25. Sacconi R, Corbelli E, Carnevali A, Querques L, Bandello F, Querques G. Optical coherence tomography angiography in geographic atrophy [published online ahead of print October 6, 2017]. *Retina*. doi:10.1097/IAE.0000000000001873.
26. Biesemeier A, Taubitz T, Julien S, Yoeruek E, Schraermeyer U. Choriocapillaris breakdown precedes retinal degeneration in age-related macular degeneration. *Neurobiol Aging*. 2014;35:2562–2573.
27. Datta S, Cano M, Ebrahimi K, Wang L, Handa JT. The impact of oxidative stress and inflammation on RPE degeneration in non-neovascular AMD. *Prog Retinal Eye Res*. 2017;60:201–218.
28. Flage T, Ringvold A. The retinal pigment epithelium diffusion barrier in the rabbit eye after sodium iodate injection. A light and electron microscopic study using horseradish peroxidase as a tracer. *Exp Eye Res*. 1982;34:933–940.
29. Sen HA, Berkowitz BA, Ando N, de Juan E Jr. In vivo imaging of breakdown of the inner and outer blood-retinal barriers. *Invest Ophthalmol Vis Sci*. 1992;33:3507–3512.
30. Zhang XY, Ng TK, Brelen ME, et al. Continuous exposure to non-lethal doses of sodium iodate induces retinal pigment epithelial cell dysfunction. *Sci Rep*. 2016;6:37279.

Investigative Ophthalmology & Visual Science